

High-Fidelity 3D Magnetic Inversion via Deep Learning-Based Geophysical Modeling

Saikat Mahato

August 23, 2025



**Under the supervision of
Dr. Anand Singh**

Department of Earth Sciences, Indian Institute of Technology Bombay, India

Second APS Presentation

Introduction

- Magnetic surveys provide key insights into the Earth's subsurface, supporting exploration, tectonic studies, and environmental investigations.
- Inversion is inherently ill-posed due to non-uniqueness of solutions, loss of resolution with depth, and high computational cost for large 3D models (Zhdanov, 2015).
- Local optimization methods risk local minima and unreliable solutions, while global optimization is more robust but computationally expensive (Bodin et al. 2012).

Introduction

- DL extracts hierarchical features directly from raw data (via CNNs, RNNs) and transforms them into meaningful representations for pattern recognition and inference.
- Medical imaging (Greenwald et al., 2022; Soomro et al., 2022)
- Natural language processing (Otter et al., 2020).
- DL methods have been applied in geophysics: electromagnetic (He et al., 2025) , seismic (Sun et al., 2021)and potential field inversion (Hu et al., 2021) .

Introduction

- Xception architecture (Chollet, 2017) has been highly successful in image recognition and related 2D vision tasks due to its efficient depthwise separable convolutions.
- It reduces parameters and computational cost while enabling strong feature extraction.

Objectives

- To develop a deep learning-based inversion framework that enhances the accuracy and efficiency of 3D magnetic inversion for subsurface characterization.
- To design and adapt Xception neural architectures for handling input-output mappings between observed magnetic data and 3D susceptibility distributions.

Methodology: Forward Modeling

- The subsurface is discretized into rectangular prisms to approximate the geology.
- Magnetic total field anomaly (TFA) is computed using the analytical solution of a rectangular prism (Bhattacharyya, 1964; Blakely, 1996).

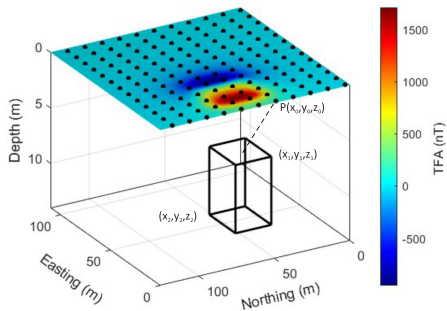


Figure :Total Field Anomaly (TFA) from a subsurface prism.
Colored map shows TFA (nT) at observation points (black dots).

Methodology: Forward Modeling

- Analytical Expression for TFA

$$\begin{aligned}\Delta T = & C_m M \left[\frac{\alpha_{23}}{2} \log \left(\frac{r - x'}{r + x'} \right) + \frac{\alpha_{13}}{2} \log \left(\frac{r - y'}{r + y'} \right) - \alpha_{12} \log(r + z_1) \right] \\ & - M_x F_x \arctan \left(\frac{x' y'}{x'^2 + r z_1 + z_1^2} \right) - M_y F_y \arctan \left(\frac{x' y'}{r^2 + r z_1 - x'^2} \right) \\ & + M_z F_z \arctan \left(\frac{x' y'}{r z_1} \right) \Big|_{\substack{x' = x_1, x' = x_2 \\ y' = y_1, y' = y_2}} \quad (1)\end{aligned}$$

- $\alpha_{12} = M_x F_y + M_y F_x$, $\alpha_{13} = M_x F_z + M_z F_x$, $\alpha_{23} = M_y F_z + M_z F_y$
- x and y = horizontal distances from prism edges to the observation point
- $r^2 = x^2 + y^2 + z^2$ = squared radial distance from a prism corner
- confirm **zt and z0**

Methodology: Conventional Inversion

- Objective function (Tikhonov, 1977):

$$\min_m \|W_d(d_{obs} - Am)\|_2^2 + \|W_m(m - m_0)\|_2^2$$

- Normal equation:

$$(A^\top W_d^\top W_d A + W_m^\top W_m) m = A^\top W_d^\top W_d d_{obs} + W_m^\top W_m m_0$$

- Data-space reformulation (Wang et al., 2015):

$$m = m_0 + W_m^{-1} A^\top (A W_m^{-1} A^\top + W_d^{-2})^{-1} (d_{obs} - Am_0)$$

- Depth weighting (Li & Oldenburg, 1996) and Cauchy norm regularization (Pilkington, 2009) improve resolution and compactness.

Methodology

Deep Learning-Based Inversion

- Estimates subsurface properties \mathbf{m} from observed data \mathbf{d} .
- Forward relation: $\mathbf{d} = G\mathbf{m} + \epsilon$.
- Inversion via CNN: $\mathbf{m} = f_\theta(\mathbf{d})$.

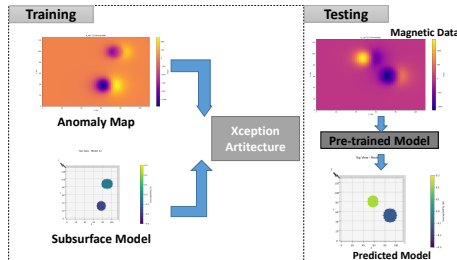


Figure: Flowchart of the CNN-based inversion process.

Methodology

Advantages once trained:

- Orders of magnitude faster predictions than conventional methods.
- Customizable for specific geophysical problems.

Recent trends:

- Use of Xception-style architectures for high-resolution 3D imaging.
- Demonstrated improvements in accuracy, scalability, and efficiency.

Methodology

Xception architecture (Chollet, 2017):

- Depthwise separable convolutions (depthwise + pointwise).
- Fewer parameters, lower computational cost.
- Retains high representational capacity.
- Efficiently learns spatial + inter-channel dependencies.

Methodology

- **Depthwise Separable Convolutions:**
 - Depthwise conv: spatial filters per channel.
 - Pointwise conv (1×1): recombines channels.
 - \Rightarrow fewer parameters, efficient, high resolution.
- Architecture stages:
 - ① Entry Flow – feature extraction + downsampling.
 - ② Middle Flow – 8 residual SepConv blocks.
 - ③ Exit Flow – upsampling + reconstruction.

Entry Flow

- Input: (56, 64, 1) magnetic anomaly map.
- Conv (32 filters, 3×3 , stride (2,2)) + BN + ReLU.
- Conv (64 filters, 3×3).
- Residual block:
 - Two SepConv layers (128 filters).
 - Shortcut: Conv (1×1 , 128 filters, stride (2,2)).
- MaxPooling (2×2).
- **Skip Connection (Skip-1)** saved for decoding.

Middle Flow

- Block repeated 8 times:
 - ReLU → SepConv (128, 3×3) → BN.
 - ReLU → SepConv (128, 3×3) → BN.
 - Residual connection: input + output.
- Preserves spatial context and ensures gradient stability.

Exit Flow

- SepConv (128) → BN → ReLU.
- Bilinear upsampling (2, 2).
- Concatenate with **Skip-1**.
- Conv layers: (128, 128, 64, 32 filters).
- Final Conv (1×1 , 15 filters) → Output (56, 64, 15) susceptibility distribution.

Training Objective

- Loss function: Mean Absolute Error (MAE)

$$L = \frac{1}{N} \sum_{i=1}^N |y_{\text{pred}}^{(i)} - y_{\text{true}}^{(i)}|$$

- Promotes robustness to noise/outliers.
- Ensures stable convergence.

Network Architecture Diagram

Activation patterns across the layers

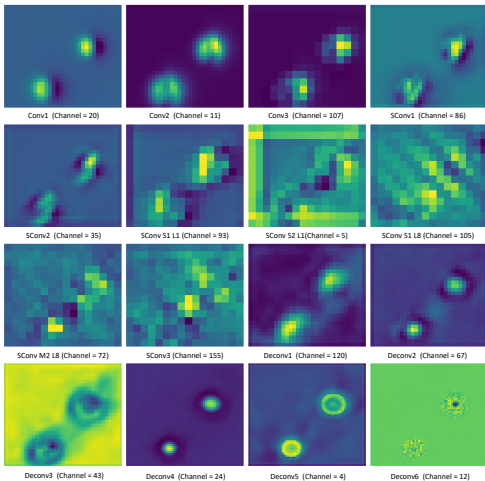


Figure : Most activated channels from various layers. Early layers show local features; deeper layers capture broader spatial patterns in geophysical data.

Results: Testing with Simple Models

- Ellipsoidal Models

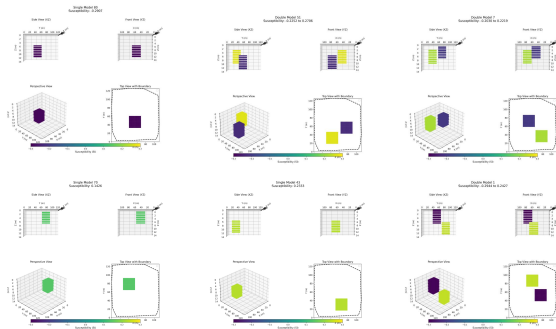


Figure: from various layers. Early layers show local features; deeper layers capture broader spatial patterns in geophysical data.

Results: Testing with Simple Models

- Cube Models

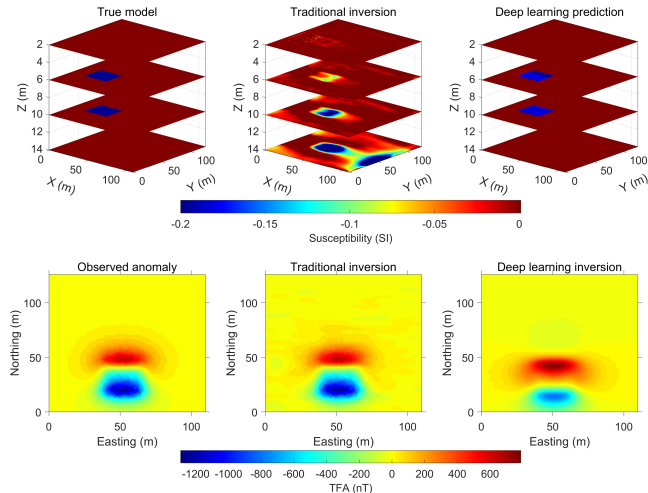


Figure: Most activated channels from various layers. Early layers show local features; deeper layers capture broader spatial patterns in geophysical data.

Results: Testing with Simple Models

- Ellipsoidal Models

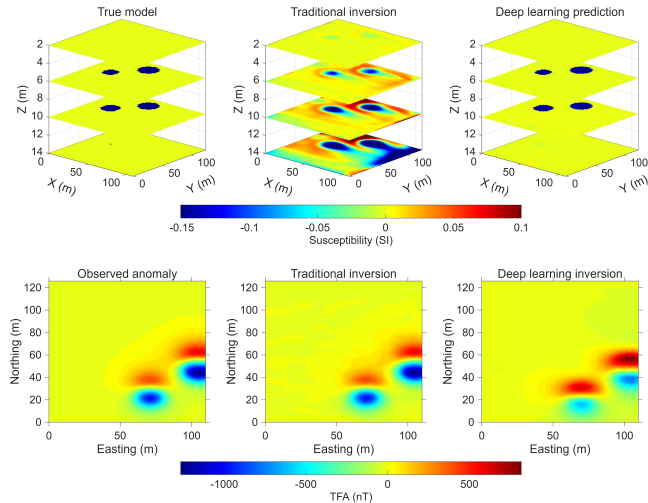


Figure: from various layers. Early layers show local features; deeper layers capture broader spatial patterns in geophysical data

Results: Testing with Simple Models

- Ellipsoidal Models

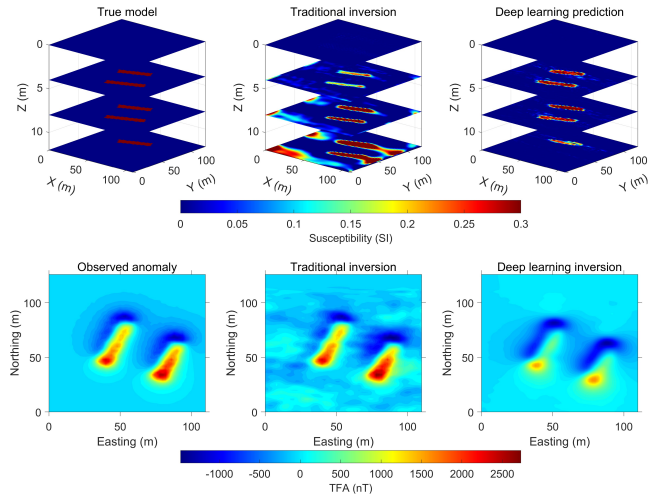
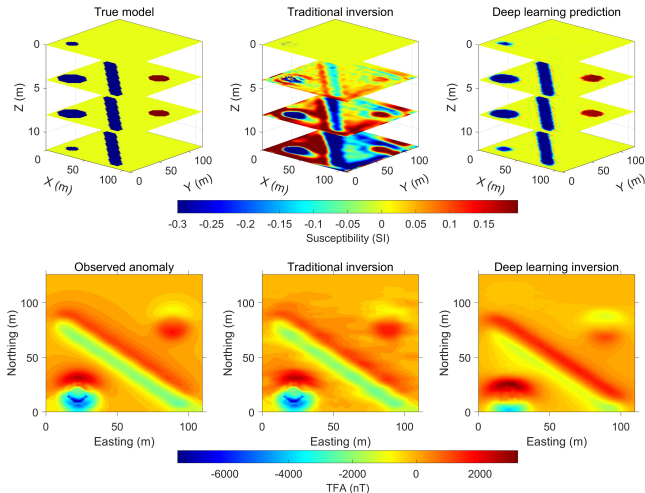


Figure: from various layers. Early layers show local features; deeper layers capture broader spatial patterns in geophysical data.

Results: Testing with Mixed Models

- Ellipsoidal Models
- Handles complex structures (dyke + ellipsoid + cuboid).



Validation

- **Loss:** Training and validation loss

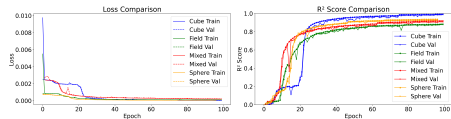
$$L = \frac{1}{N} \sum (y_{true} - y_{pred})^2$$

Validation loss is computed on unseen data after each epoch.

- **R^2 Score:**

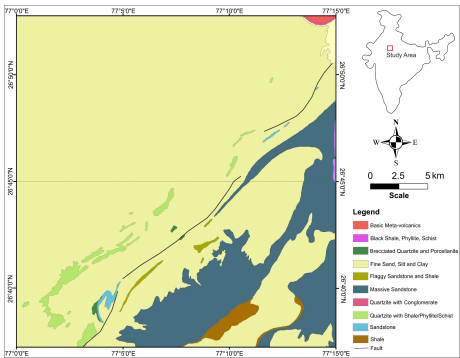
$$R^2 = 1 - \frac{\sum (y_{true} - y_{pred})^2}{\sum (y_{true} - \bar{y})^2}$$

Measures prediction quality ($R^2 \approx 1$ = better fit).
Computed on validation dataset.



Field Application

- The subsurface is discretized into rectangular prisms to approximate the geology.
- Magnetic total field anomaly (TFA) is computed using the analytical solution of a rectangular prism (Bhattacharyya, 1964; Blakely, 1996).



Conclusion

- The observed TFA map, shown in Figure S8, reveals three prominent magnetic anomalies each characterized by a pronounced peak in intensity, most likely indicative of distinct magnetic bodies or zones of fracturing within the subsurface.
- Synthetic models were designed with their initial positioning and orientation directly informed by these anomaly locations, establishing a direct link between data-driven feature selection and the crafting of training examples.
- To ensure the inversion model could generalize to a realistic range of possible geological scenarios rather than being narrowly tuned to a few idealized cases, the modeling workflow deliberately introduced extensive structural diversity and augmentation into the forward modeling process.

Observed TFA Map Insights

Revealed three prominent magnetic anomalies with high-intensity peaks.
Likely indicate distinct magnetic bodies or fractured zones.

References

- Bhattacharyya, B. (1964). Magnetic anomalies due to prism-shaped bodies...
- Chollet, F. (2017). Xception: Deep learning with depthwise separable convolutions...